Population Pharmacokinetics and Target Attainment of Ertapenem in Plasma and Tissue Assessed via Microdialysis in Morbidly Obese Patients after Laparoscopic Visceral Surgery

Mathias Wittau,[a] Stephan Paschke,[a] Max Kurlbaum,[b*] Jan Scheele,[a]
Neang S. Ly,[c*] Evelyn Hemper,[a] Marko Kornmann,[a] Doris Henne-Bruns,[a]
Jürgen B. Bulitta[d]

Department of Visceral Surgery, University of Ulm, Ulm, Germany[a]; Department of Clinical Chemistry, University of Ulm, Ulm, Germany[b]; School of Pharmacy and Pharmaceutical Sciences, University at Buffalo, State University of New York, Buffalo, New York, USA[c]; Center for Pharmacometrics and Systems Pharmacology, Department of Pharmaceutics, College of Pharmacy, University of Florida, Orlando, Florida, USA[d]

ABSTRACT Ertapenem provides broad-spectrum activity against many pathogens, and its use is relevant for the prophylaxis and treatment of infections in morbidly obese patients undergoing surgery. However, its pharmacokinetics and tissue penetration in these patients are not well defined. We assessed the population pharmacokinetics and target attainment for ertapenem in the plasma, subcutaneous tissue, and peritoneal fluid of morbidly obese patients. Six female patients (body mass index, 43.7 to 55.9 kg/m^2) received 1,000 mg ertapenem as 15-min infusions at 0 and 26 h. On day 2, the unbound ertapenem concentrations in plasma, subcutaneous tissue, and peritoneal fluid were measured by microdialysis; total plasma concentrations were additionally quantified. The probability of attaining a target of an unbound ertapenem concentration above the MIC for at least 40% of the dosing interval was predicted via Monte Carlo simulations. The population pharmacokinetic model contained two disposition compartments and simultaneously described all concentrations. For unbound ertapenem, total clearance was 12.3 liters/h (coefficient of variation, 21.6% for between-patient variability) and the volume of distribution at steady state was 57.8 liters in patients with a 53-kg fat-free mass. The area under the concentration-time curve (AUC) for ertapenem was 49% lower in subcutaneous tissue and 25% lower in peritoneal fluid than the unbound AUC in plasma. Tissue penetration was rapid (equilibration half-life, <15 min) and was variable in subcutaneous tissue. Short-term ertapenem infusions (1,000 mg every 24 h) achieved robust (>90%) target attainment probabilities for MICs of up to 1 mg/liter in plasma, 0.25 to 0.5 mg/liter in subcutaneous tissue, and 0.5 mg/liter in peritoneal fluid. Ertapenem presents an attractive choice for many pathogens relevant to morbidly obese patients undergoing surgery. (This study has been registered at ClinicalTrials.gov under identifier NCT01407965.)

KEYWORDS ertapenem, morbidly obese patients, population pharmacokinetics, subcutaneous tissue, microdialysis, S-ADAPT, Monte Carlo simulation, pharmacodynamics

Ertapenem covers many bacterial pathogens, and its use is relevant for the prophylaxis and treatment of infections in morbidly obese patients undergoing laparoscopic visceral surgery (1). Ertapenem has a relatively high level of protein binding

compared to that of the other carbapenems and, therefore, also has a longer terminal half-life (2, 3). The long half-life of ertapenem provides clinicians more flexibility regarding the timing of doses and potential redosing than they have with other β-lactams (4–8). Thus, ertapenem may be attractive for use in this patient population.

While ertapenem may be a valuable treatment option for patients with intra-abdominal infections, its pharmacokinetic (PK)/pharmacodynamic (PD) profile needs to be carefully evaluated, as the risk for hospital-related and postoperative infections is considerable (9). This is particularly problematic for morbidly obese patients, in whom a small skin lesion can remain unnoticed, may become infected, and, if it remains untreated, may turn into a life-threatening infection.

Previous studies showed the extensive penetration of ertapenem into blister fluid in healthy volunteers (10) and into peritoneal fluid in patients requiring intra-abdominal surgery (11). Likewise, penetration into the peritoneal fluid of patients on continuous ambulatory peritoneal dialysis is substantial (12). The median area under the concentration-time curve (AUC) in peritoneal fluid divided by the total ertapenem AUC in plasma was 0.801 (interquartile range, 0.486 to 1.317). Extensive penetration of ertapenem was also found for colorectal and intra-abdominal tissues (13, 14), bone (15), and lung epithelial lining fluid (16, 17). As none of these tissue penetration studies assessed obese patients, it is essential to ensure that antibiotic coverage during and after surgery in morbidly obese patients is adequate to achieve beneficial clinical outcomes (9, 18).

Antibiotic dosing regimens are most commonly optimized on the basis of data for nonobese patients (including data for healthy volunteers). As morbidly obese patients may have considerably altered PK and tissue penetration compared to nonobese patients, it seems critical to optimize dosing regimens for morbidly obese patients. The extensive amount of body fat in morbidly obese patients has the potential to significantly alter penetration into subcutaneous tissue. Moreover, the lifestyle of morbidly obese patients is likely associated with a decreased amount of physical activity compared to that in healthy volunteers. Therefore, it is important to evaluate a suitable body size descriptor for dosing of morbidly obese patients.

We considered both total body weight (WT) and fat-free mass (FFM) to characterize body size and body composition and to scale clearance and the volume of distribution (4, 19). Suboptimal dosing regimens in obese patients may lead to clinical failures, complications with surgery, and the emergence of bacterial resistance.

Population PK modeling is arguably the most powerful methodology for the simultaneous characterization of the time course of drug concentrations in plasma and tissues. The PK of ertapenem in obese patients (body mass index [BMI], $\geq$40 kg/m^2) has been determined in only two studies with sample sizes of 10 patients in each study (20, 21). When clearance was scaled by total body weight or by body surface area, Chen et al. (20) found that clearances in class I and II obese patients and class III obese patients were lower than those in healthy volunteers. This suggested that neither of these body size measures explains the difference in PK between healthy volunteers and obese patients. The noncompartmental total clearance estimate (in liters per hour per kilogram of body weight) for class III obese patients reported by Borracci et al. (21) was similar to that reported by Chen et al. (20). These studies measured the total but not the unbound ertapenem plasma concentrations. As the level of plasma protein binding of ertapenem is relatively high and concentration dependent (3, 14, 22), measurement of the unbound concentrations in plasma and tissues may help to optimize dosing regimens. We are also not aware of studies on the tissue penetration of ertapenem in obese patients.

Thus, the primary objective of this study was to determine the population PK of unbound ertapenem in the plasma, peritoneal fluid, and subcutaneous tissue of morbidly obese, noninfected subjects. Our second objective was to predict the probability of target attainment for ertapenem in this patient group via Monte Carlo simulations.

TABLE 1 Demographic characteristics[a]

Characteristic	Avg ± SD	Median (range)
Age (yr)	43.2 ± 14.7	44 (27–59)
Wt (kg)	139 ± 29.6	131 (109–182)
FFM (kg)	60.9 ± 9.47	57.2 (51.3–75.5)
Ht (cm)	166 ± 9.69	162 (156–181)
BMI (kg/m^2)	50.1 ± 5.74	50.5 (43.7–55.9)
Body surface area (m^2)	2.52 ± 0.336	2.41 (2.17–3.02)
Serum protein concn (g/liter)	71.3 ± 1.71	71.5 (69.0–73.0)
Serum creatinine concn (μmol/liter)	62.3 ± 9.63	59.5 (54.0–81.0)
Albumin concn (g/liter)	40.2 ± 3.54	38.5 (37.0–46.0)

[a]Data are for six females.

RESULTS

This study comprised six morbidly obese female subjects. The mean ± standard deviation (SD) body weight was 139 ± 29.6 kg, and BMI was 50.1 ± 5.74 kg/m^2 (Table 1). Noncompartmental analysis yielded a terminal half-life of 4.46 ± 0.84 h for total drug and 3.95 ± 0.95 h for unbound ertapenem in plasma. Peak concentrations were 83.0 ± 17.1 mg/liter for total drug and 19.4 ± 4.38 mg/liter for unbound ertapenem in plasma, 12.5 ± 5.21 mg/liter for unbound ertapenem in subcutaneous tissue, and 16.1 ± 0.767 mg/liter for unbound ertapenem in peritoneal fluid ($n = 5$, due to the loss of the peritoneal catheter in one patient). The median for the number of quantifiable concentrations per patient was 7 (range, 5 to 8) for peritoneal fluid and 3 (range, 2 to 8) for subcutaneous tissue (Fig. 1). The results of microdialysis obtained with these serial tissue samples support the population PK modeling.

The final population PK model yielded individual parameter estimates of a median of 13.0 liters/h (range, 11.6 to 19.2 liters/h) for total clearance and 62.5 liters (range, 58.5 to 85.5 liters) for the volume of distribution at steady state. These individual estimates are slightly larger than the population means shown in Table 2, as the population means were scaled to a standard FFM of 53 kg. Ertapenem plasma and tissue concentrations declined biexponentially (Fig. 1), and plasma concentrations were best described by a two-compartment model (Fig. 2). The variability of the concentrations observed in subcutaneous tissue was larger than that of the concentrations observed in peritoneal fluid. In total, five tissue concentrations were excluded from the final modeling analysis, since these concentrations declined with a much shorter half-life than the plasma concentrations in the respective subject. As all five of these concentrations were determined at the end of the sampling period, these rapidly declining tissue concentrations might have been caused by a degradation of the dialysis membrane over time. In an additional analysis which contained these five tissue concentrations, the population means for the ratio of the unbound AUC in subcutaneous tissue divided by the unbound AUC in plasma (F_{SC}) and for the ratio of the unbound AUC in peritoneal fluid divided by the unbound AUC in plasma (F_{PF}) were slightly lower than the estimates of the final model: for F_{SC}, 0.459 and 0.507, respectively, and for F_{PF}, 0.742 and 0.754, respectively (Table 2). This suggested that this modeling decision had only a minor impact on the overall modeling results.

Overall, the individual fitted versus observed concentrations had coefficients of correlation of 0.99 for the total and unbound concentrations in plasma, 0.80 for unbound concentrations in subcutaneous tissue, and 0.93 for unbound concentrations in peritoneal fluid.

The population mean clearance for unbound ertapenem was 12.3 liters/h and the volume of distribution was 57.8 liters for subjects with a mean FFM of 53 kg (Table 2). Population mean estimates were reasonably precise, with relative standard errors being below 42% for all parameters (except for the small linear binding component). Between-subject variability (BSV) was 26% or less for all disposition parameters. While the subcutaneous tissue concentrations were more variable (coefficient of variation [CV], 41.8%), the variability for peritoneal fluid was small (CV, <5%). As expected, the
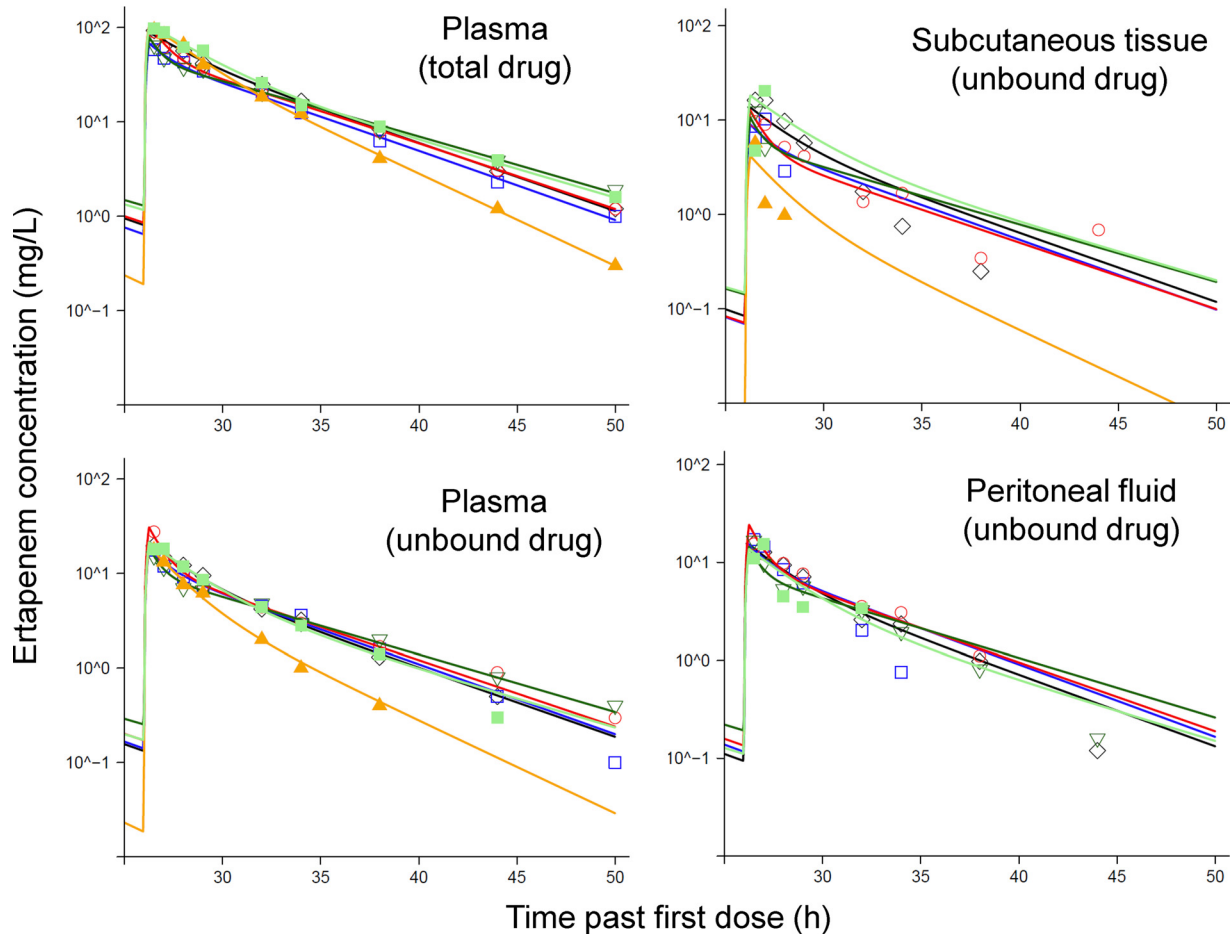
FIG 1 Observed (markers) and individually fitted (lines) ertapenem concentrations in plasma (unbound and total drug) and unbound ertapenem concentrations in subcutaneous tissue and peritoneal fluid after 1,000 mg of ertapenem was dosed as 15-min infusions at 0 and 26 h. All panels except the panel for peritoneal fluid show the profiles for six subjects; the panel for peritoneal fluid shows the profiles for five subjects.

relative standard errors for the between-subject variability estimates were larger than those for the population means (Table 2), especially for parameters estimated with a small between-subject variability (i.e., coefficient of variation, <10%). The larger relative standard errors of the between-subject variability had a limited impact on the predictions from the final model, since the visual predictive checks indicated adequate predictive performance (see Fig. S1 in the supplemental material).

Relative to the unbound ertapenem exposure (i.e., AUC) in plasma, the average drug exposure was 50.7% for subcutaneous tissue and 75.4% for peritoneal fluid (Table 2). Modeling showed that the rate of tissue penetration was rapid. When we applied the most flexible approach (i.e., the third approach) to estimate the rate and extent of tissue penetration, the estimated mean equilibration half-lives were less than 15 min. Compared to the simplest approach (i.e., the first approach [see Materials and Methods]) of estimating tissue penetration for ertapenem, neither the objective function ($-1 \cdot \log$ likelihood) nor the diagnostic plots improved. Thus, we assumed a rapid tissue penetration of ertapenem (Fig. 2). Visual predictive checks indicated an adequate predictive performance for all four dependent variables (Fig. S1). The central tendency was adequately captured by the median simulated concentrations, whereas the predicted variability was slightly wider than the variability of the observations. This leads to slightly lower (i.e., conservative) predicted PK/PD breakpoints. The individual fitted versus observed plasma concentrations were precise and unbiased (Fig. S2), whereas the individual fits for subcutaneous tissue and peritoneal fluid were less precise. The population fitted concentrations were unbiased (Fig. S3) and, as expected, less precise.

TABLE 2 Population PK parameter estimates for ertapenem in morbidly obese patients[e]

Parameter	Abbreviaton	Units	Population mean (relative SE [%])	Between-subject variability (relative SE [%])
Total clearance	CL^a	liters/h	12.3[a] (9.0)	0.216[c] (71.3)
Distribution clearance between central and peripheral compartments	CLd^a	liters/h	7.49[a] (39.7)	0.261 (199)
Volume of distribution of central compartment	V_1^a	liters	40.0[a] (7.4)	0.110 (85.5)
Volume of distribution of peripheral compartment	V_2^a	liters	17.8[a] (18.7)	0.0598 (431)[d]
Ratio of unbound AUC in subcutaneous tissue/unbound AUC in plasma	F_{SC}		0.507[b] (21.6)	0.418 (104)
Ratio of unbound AUC in peritoneal fluid/ unbound AUC in plasma	F_{PF}		0.754[b] (9.5)	0.0182 (1,339)[d]
Linear binding component in plasma	B_{lin}		0.185 (121)	0.335 (279)
Dissociation constant for saturable binding	K_d	mg/liter	32.1 (41.8)	0.0620 (1,090)[d]
Ratio of maximum binding capacity and K_d	B_{sat}/K_d		4.91 (12.3)	0.266 (70.4)

[a]Estimates represent a patient with a normal body size (i.e., a 53-kg fat-free mass) and are based on an allometric body size model with fixed exponents of 0.75 for clearances and 1.0 for volumes of distribution.

[b]The half-life of equilibration between subcutaneous tissue and plasma and between peritoneal fluid and plasma was rapid (equilibration half-life, <15 min). The final model assumed a rapid equilibration between the respective peripheral site and plasma.

[c]This estimate represents the apparent coefficient of variation of a normal distribution on a natural logarithmic scale.

[d]The relative standard error refers to the estimated variance. For parameters with a small estimated between-subject variability (i.e., coefficient of variation less than 10%), the relative standard error was large, because the estimated variance was very small. Thus, large relative standard errors were expected for parameters with a low between-subject variability and a study with a small sample size. This did not impact the predictive performance of the model, which was assessed via visual predictive checks.

[e]AUC, area under the concentration-time curve from time zero to infinity. The standard deviations of the additive and proportional residual error were 0.00844 mg/ liter and 8.48%, respectively, for unbound ertapenem in plasma, 0.109 mg/liter and 10.4%, respectively, for total ertapenem in plasma, 0.227 mg/liter and 40.2%, respectively, for unbound drug in subcutaneous tissue, and 0.165 mg/liter and 22.9%, respectively, for unbound drug in peritoneal fluid.

Monte Carlo simulations predicted a breakpoint of 2 mg/liter in plasma, 0.5 mg/liter in subcutaneous tissue, and 1 mg/liter in peritoneal fluid for a continuous infusion of ertapenem at 1 g per day (plus a 500-mg loading dose given as a 15-min infusion at 0 h) (Fig. 3). For a short-term infusion of 1 g every 24 h, the PK/PD breakpoints for a target of a duration of unbound ertapenem plasma concentrations above the MIC at steady
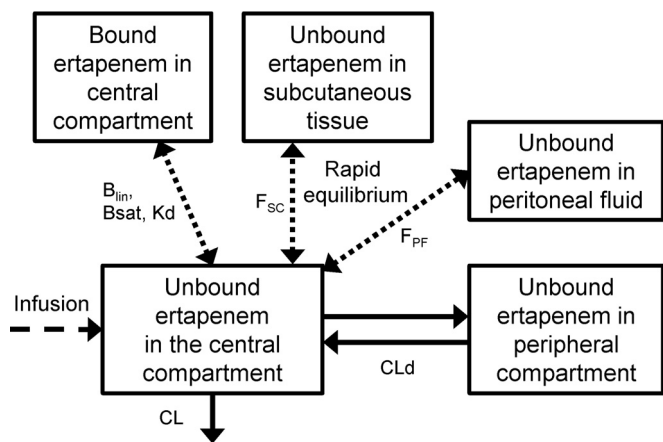

FIG 2 Structure of the final model for unbound and bound ertapenem in plasma and unbound ertapenem in subcutaneous tissue and peritoneal fluid. The model contained a central compartment and a peripheral compartment as well as one compartment each for bound ertapenem in plasma and for unbound ertapenem in subcutaneous tissue and peritoneal fluid. The ertapenem concentrations in the last three compartments were in rapid equilibrium with the unbound ertapenem concentrations in the central compartment. The unbound ertapenem concentrations in tissue were assumed to not affect or to only minimally affect the overall disposition of ertapenem (i.e., the amount of drug in the central and peripheral compartments). B_{lin}, linear binding component in plasma; B_{sat}, saturable binding component in plasma; K_d, dissociation constant for saturable binding; F_{SC}, ratio of the unbound AUC in subcutaneous tissue divided by the unbound AUC in plasma; F_{PF}, ratio of the unbound AUC in peritoneal fluid divided by the unbound AUC in plasma; CL, total clearance; CLd, distribution clearance between the central and peripheral compartment.
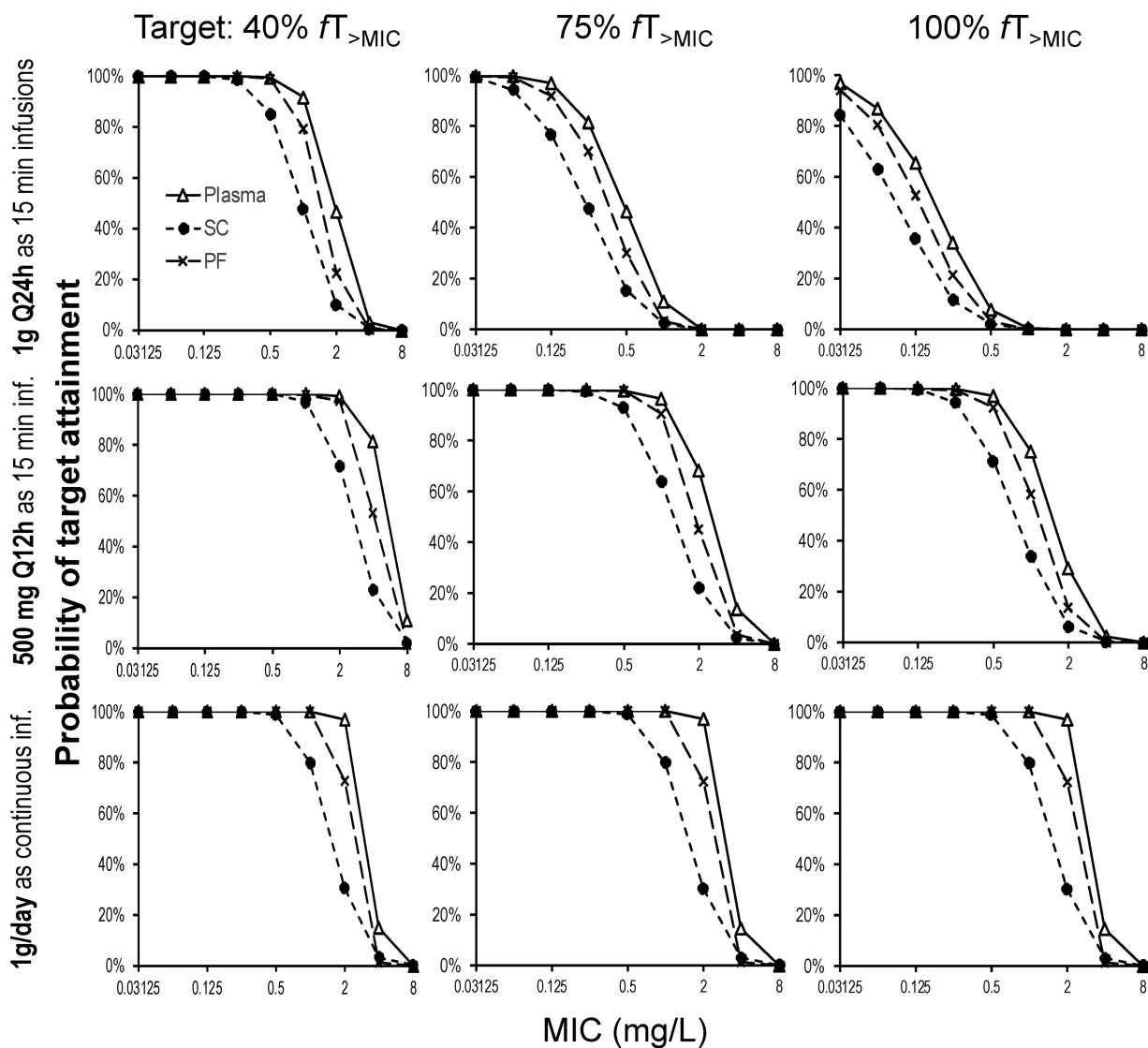
FIG 3 Probabilities of target attainment for 1 g of ertapenem dosed as a 15-min infusion (inf.) of 1,000 mg every 24 h (Q24h), as a 15-min infusion of 500 mg every 12 h (Q12h), or as a continuous infusion of 1,000 mg/day with a 500-mg loading dose at 0 h. The PK/PD targets of an fT_{MIC} of 40%, 75%, and 100% were utilized for the ertapenem concentrations in plasma, subcutaneous tissue (SC), and peritoneal fluid (PF).

state expressed as a fraction of the dosing interval (fT_{MIC}) of 40% were 1 mg/liter in plasma, 0.25 mg/liter in subcutaneous tissue, and 0.5 mg/liter in peritoneal fluid. As expected, for the fT_{MIC} target of 75%, breakpoints were considerably lower for short-term infusions of 1 g every 24 h (0.125 mg/liter in plasma, 0.0625 mg/liter in subcutaneous tissue, and 0.125 mg/liter in peritoneal fluid). When ertapenem was given at 500 mg every 12 h, ertapenem breakpoints were more similar to those for the continuous infusion (Fig. 3).

DISCUSSION

Obesity is a growing global problem in developed and developing countries (23). It is considered a chronic disease with pandemic proportions. Thus, obesity is one of the greatest threats to human health, and the number of surgeries in morbidly obese patients continues to increase worldwide. Unfortunately, obese patients are at a higher risk of postoperative and hospital-related infections (9). Selection of an antibiotic which covers the microbial spectrum and has adequate tissue penetration is crucial for both antibiotic prophylaxis and therapy. Ertapenem is an attractive β-lactam antibiotic due to its relatively long terminal half-life (4 to 5 h, on average) and activity against many

pathogens relevant for superficial incisional surgical site infections (SSIs), deep incisional SSIs, and organ space SSIs in morbidly obese patients, e.g., *Staphylococcus* spp. and *Streptococcus* spp. (24). Further, ertapenem covers most of the common microbial spectrum found in intra-abdominal infections with peritonitis (25, 26). However, the free ertapenem concentration in the subcutaneous tissue and peritoneal fluid of morbidly obese patients has not yet been characterized. Ertapenem is approved for the use in patients at a dose of 1,000 mg every 24 h. The approval and the dosing recommendation were mainly based on studies in healthy, nonobese volunteers (27).

This study presents the first population PK analysis of ertapenem in morbidly obese patients based on total and unbound concentrations in plasma and the unbound drug concentration in subcutaneous tissue and peritoneal fluid. The unbound drug exposure in subcutaneous tissue was variable and approximately 50.7% of the unbound AUC in plasma. Unbound drug exposure in peritoneal fluid was 75.4% of that in plasma and less variable than the penetration into subcutaneous tissue (Table 2).

The AUC of unbound ertapenem in muscle tissue divided by the total drug AUC in plasma was 13% $\pm$ 9% in healthy volunteers (28). For subcutaneous tissue, this ratio was 5% $\pm$ 1%. After accounting for the 90% protein binding determined in this study, the AUC for unbound ertapenem in tissue divided by the AUC for unbound ertapenem in plasma would be approximately 130% for muscle and 50% for subcutaneous tissue. Compared to the AUC ratios in the previous study (28), our AUC ratios in morbidly obese patients were very similar for subcutaneous tissue (F_{SC}, 50.7%; Table 2) and slightly lower for peritoneal fluid (F_{PF}, 75.4%). The ertapenem penetration into soft tissue adjacent to a foot infection in diabetic patients was well comparable to these results. The unbound AUC in tissue divided by the total drug AUC in plasma was 8.3% for healthy tissue and 9.5% for inflamed tissue (29). Assuming a protein binding of 90% in plasma, this would translate into unbound AUC ratios of approximately 83% and 95%, respectively. Penetration into these tissues was rapid, similar to the findings of our study. Likewise, the penetration of ertapenem into muscle in mechanically ventilated patients was rapid, and the AUC for unbound ertapenem in muscle tissue divided by the total drug AUC in plasma was 9% $\pm$ 5% (mean $\pm$ SD) (30). Overall, the findings of these and the present tissue penetration studies were in good agreement.

Owing to the variable and low penetration into subcutaneous tissue, the PK/PD breakpoints were approximately 2- to 4-fold lower in subcutaneous tissue than in plasma; the breakpoints for peritoneal fluid were between those for subcutaneous tissue and plasma. Dosing short-term infusions of 500 mg every 12 h resulted in considerably higher breakpoints than dosing of 1 g every 24 h. This was particularly true for fT_{MIC} targets of 75% and 100%. Short-term infusions of 500 mg every 12 h reached almost the same breakpoints as a continuous ertapenem infusion of 1 g per day (with a small loading dose). Our breakpoints were slightly higher than those reported previously by Chen et al. (20) for ertapenem in obese healthy volunteers. The latter study assumed a 95% protein binding for Monte Carlo simulations, whereas we quantified and modeled unbound ertapenem concentrations. This could have contributed to the slightly higher breakpoints in our study.

The comparison of the EUCAST MIC_{50} and MIC_{90} with the PK/PD breakpoints for standard and optimized dosing regimens yielded three groups of pathogens relevant to infections in morbidly obese patients. For the first group (Table 3), all dosing regimens covered the EUCAST MIC_{90}, suggesting that standard therapy is expected to be sufficient. Optimized dosing regimens (i.e., a continuous infusion of 1 g per day or dosing of 0.5 g ertapenem as a short-term infusion every 12 h) covered the MIC_{90}, whereas standard short-term infusions tended to cover only the MIC_{50}, depending on the infection site (Table 3). The third group contained pathogens like *Acinetobacter baumannii* and *Staphylococcus epidermidis*, which are not reliably covered by any ertapenem dosing regimen.

Our final population PK model yielded adequate curve fits (Fig. 2) and had good predictive performance (see Fig. S1 in the supplemental material). Modeling showed that the rate of penetration of ertapenem into subcutaneous tissue and peritoneal fluid

TABLE 3 Comparison of the susceptibility data from the EUCAST MIC distribution (MIC$_{50}$ and MIC$_{90}$) with the PK/PD breakpoints for the f T$_{MIC}$ targets of 40% and 75% for standard and optimized dosing regimens at 1 g ertapenem per day[c]

MIC$_{90}$ coverage and pathogen (no. of isolates in EUCAST database)	EUCAST[a] MIC$_{50}$ (mg/liter)	MIC$_{90}$ (mg/liter)	fTMIC target of 40% (1 g as a 15-min infusion q24h) Plasma (1 mg/liter)[b]	SC (0.25 mg/liter)	PF (0.5 mg/liter)	f T$_{MIC}$ target of 75% — 1 g as a 15-min infusion q24h Plasma (0.125 mg/liter)	SC (0.0625 mg/liter)	PF (0.125 mg/liter)	0.5 g as a 15-min infusion q12h Plasma (1 mg/liter)	SC (0.5 mg/liter)	PF (1 mg/liter)	1 g as a continuous infusion Plasma (2 mg/liter)	SC (0.5 mg/liter)	PF (1 mg/liter)
MIC$_{90}$ is covered for all regimens and sites														
Proteus mirabilis (n = 1,426)	0.008	0.016	+++	+++	+++	+++	+++	+++	+++	+++	+++	+++	+++	+++
Escherichia coli (n = 2,187)	0.008	0.031	+++	+++	+++	+++	+++	+++	+++	+++	+++	+++	+++	+++
Klebsiella spp. (n = 342)	0.016	0.031	+++	+++	+++	+++	+++	+++	+++	+++	+++	+++	+++	+++
Streptococcus pyogenes (n = 818)	0.016	0.031	+++	+++	+++	+++	+++	+++	+++	+++	+++	+++	+++	+++
Klebsiella pneumoniae (n = 1,482)	0.016	0.063	+++	+++	+++	+++	+	+++	+++	+++	+++	+++	+++	+++
MIC$_{90}$ is better covered by optimized regimens														
Proteus vulgaris (n = 317)	0.016	0.125	+++	+++	+++	+++	+	+++	+++	+++	+++	+++	+++	+++
Streptococcus viridans group (n = 335)	0.063	0.25	+++	+++	+++	+	+	+	+++	+++	+++	+++	+++	+++
Enterobacter cloacae (n = 1,185)	0.063	1	+++	+	+	+	+	+	+++	+	+++	+++	+	+++
Enterobacter spp. (n = 255)	0.063	1	+++	+	+	+	+	+	+++	+	+++	+++	+	+++
Staphylococcus aureus (n = 1,071)	0.125	1	+++	+	+	+	NC	+	+++	+	+++	+++	+	+++
MIC$_{90}$ is not covered reliably by any regimen														
Bacteroides fragilis (n = 296)	0.25	2	+	+	+	NC	NC	NC	+	+	+	+++	+	+
Bacteroides fragilis group (n = 147)	0.5	4	+	NC	+	NC	NC	NC	+	+	+	+	+	+
Staphylococcus epidermidis (n = 203)	1	128	+	NC	NC	NC	NC	NC	+	NC	+	+	NC	+
Acinetobacter baumannii (n = 719)	4	16	NC	NC	NC	NC	NC	NC	NC	NC	NC	NC	NC	NC
Enterococcus faecalis (n = 1,183)	8	512	NC	NC	NC	NC	NC	NC	NC	NC	NC	NC	NC	NC
Enterococcus faecium (n = 325)	256	256	NC	NC	NC	NC	NC	NC	NC	NC	NC	NC	NC	NC

[a]As of 5 September 2016.
[b]Numbers in parentheses are the PK/PD breakpoints for the respective dosing regimen and site.
[c]q24h, every 24 h; SC, subcutaneous tissue; PF, peritoneal fluid; +++, the MIC$_{90}$ is covered; +, the MIC$_{50}$ is covered; NC, not covered.

was rapid, similar to the results of our previous study on meropenem in morbidly obese patients (4). While our microdialysis sampling times were not specifically selected to estimate rapid tissue penetration, these tissue sampling times allowed adequate characterization of the terminal half-life and, therefore, were adequate for predicting the fT_{MIC}.

The parameter estimates for the saturable binding of ertapenem in plasma (Table 2) were in good agreement with those from a previous population PK analysis of ertapenem in patients requiring colorectal surgery (14). Our population PK parameter estimates apply to unbound ertapenem. Due to the saturable protein binding of ertapenem in plasma, the estimates in Table 2 are not directly comparable to the PK parameter estimates for total ertapenem reported previously for obese subjects (20, 21).

The between-subject variability had a 21.6% coefficient of variation for total clearance of unbound ertapenem, and the volume of distribution was less variable. In the absence of a healthy volunteer control group, we used FFM instead of WT to describe body size and body composition in our morbidly obese patients, as we did in our previous study (4). Our study was too small to evaluate different measures of body size, such as FFM or lean body mass; FFM has previously been evaluated and found to be suitable for use in the determination of the doses of drugs of other classes to be used for obese patients (19, 31–33).

A limitation of our study was the small sample size of six morbidly obese patients, which may not have allowed us to fully capture the variability in this subject group. To describe the variability associated with body size, our Monte Carlo simulations included the between-subject variability of FFM, which had a CV of 15.5% (Table 1). This affected the variability of the clearances and volumes of distribution. Another limitation of our study was the lack of established PK/PD targets for subcutaneous tissue and peritoneal fluid. While we simulated potential fT_{MIC} targets ranging from 40% to 100%, the Monte Carlo simulation results for both tissue sites should be interpreted conservatively.

In summary, ertapenem exposure was lower and more variable for subcutaneous tissue than for peritoneal fluid when the levels of exposure in both of these compartments were compared to the exposure achieved with unbound ertapenem in plasma. Therefore, the PK/PD breakpoints were approximately 2- to 4-fold lower for subcutaneous tissue than for plasma. Dosing of ertapenem as a short-term infusion of 500 mg every 12 h or as a continuous infusion of 1 g per day was predicted to achieve approximately 8-fold higher PK/PD breakpoints for the fT_{MIC} target of 75% compared to dosing 1 g every 24 h.

Overall, for antibiotic prophylaxis related to laparoscopic visceral surgery or treatment of intraperitoneal infections in morbidly obese patients, ertapenem appears to be an attractive choice, especially when applying a dosing regimen of 500 mg every 12 h or 1 g per day as a continuous infusion. Now that the present study has ensured the adequate and rapid penetration of ertapenem into subcutaneous tissue and peritoneal fluid, future studies are warranted to assess the clinical effectiveness of ertapenem in this patient population.

MATERIALS AND METHODS

Study design. This prospective, single center, open-label study was performed at the University of Ulm, Department of Visceral Surgery, from October 2013 to July 2015 (ClinicalTrials registration no. NCT01407965). The protocol was approved by the ethics committee of the University of Ulm and The Federal Institute for Drug and Medical Devices of Germany. Prior written informed consent was obtained from all study participants. The study was performed following the recommendations from the revised version of the Declaration of Helsinki and current revisions of the Good Clinical Practice Guidelines of the European Commission.

Patient population. Noninfected, hospitalized patients aged 18 years or older with a body mass index (BMI) of at least 40 kg/m² were included. These patients required surgical intervention (open or laparoscopic surgery) at intra-abdominal organs. Exclusion criteria were lactation or pregnancy in women, a history of serious allergy or intolerance to ertapenem or other β-lactam antibiotics, emergency surgery, and systemic antimicrobial therapy with ceftazidime within 7 days prior to study entry. Additional exclusion criteria were ongoing intra-abdominal infections, terminal illness, severe diseases of the liver (e.g., cirrhosis of the liver with alanine aminotransferase or aspartate aminotransferase levels >6

times the upper limit of normal [ULN] and bilirubin levels >3 times the ULN), severe renal insufficiency with a creatinine clearance of ≤30 ml/min, a platelet count of <75,000 cells/mm³, a neutrophil count of <1,000 cells/mm³, and coagulation studies providing international normalized ratios of >1.5 times the ULN, ongoing chemotherapy and/or radiotherapy, and concurrent medication with valproic acid.

Dosing. All patients received 1,000 mg ertapenem (Invanz; license no. EU/1/02/216/001+/002; Infectopharm, Heppenheim, Germany) as 15-min intravenous infusions at 0 and 26 h on the day of surgery. After administration of the dose at 26 h, serial blood samples were obtained to characterize the PK of ertapenem. This dose was administered after the microdialysis recovery procedure and washout of the microdialysis probes (see below).

Microdialysis. Subcutaneous adipose interstitial space fluid and peritoneal fluid were sampled via microdialysis. A microdialysis probe was placed in the subcutaneous tissue of the abdominal wall after laparoscopy (63 MD; mdiaylsis, Stockholm, Sweden), and a second microdialysis probe was placed into the abdominal cavity at the end of the laparoscopic procedure (62 MD; mdiaylsis, Stockholm, Sweden). The retrodialysis technique was used to calibrate all catheters (34). The probes were perfused with lactated Ringer's solution for 24 h at a flow rate of 2 μl/min. At 24 h after the first ertapenem dose, catheters were perfused with 20 mg/liter ertapenem in lactated Ringer's solution for 60 min. A sample was collected during the last 25 min of the retrodialysis procedure, and the percent recovery was calculated as 100% ° [1 − ($C_{dialysate}$/$C_{perfusate}$)], where $C_{perfusate}$ is the initial concentration of ertapenem in the solution entering the microdialysis probe and $C_{dialysate}$ is the concentration of ertapenem in the solution leaving the probe (34). A period of washout with blank lactated Ringer's solution of at least 60 min followed the recovery procedure. Samples were obtained by microdialysis over 25 min at 30, 60, 120, 180, 360, 480, 720, 1,080, and 1,440 min after ertapenem administration. The flow rate was 2 μl/min. All samples were stabilized (see below) with 2-(4-morpholino)ethanesulfonic acid (MES; 0.100 M; pH 6.5; 1:1), immediately frozen, and stored at −80°C until analysis.

Blood sampling. Blood samples were obtained at the same times as the microdialysis samples. Blood samples were taken and immediately cooled in an ice-water bath, followed by centrifugation of blood samples at 4,000 rpm for 10 min at 4°C. Plasma samples were immediately stabilized with MES buffer (0.100 M; pH 6.5; 1:1 [vol/vol]). Matrix controls, internal standards, calibration curve standards, and samples for pharmacokinetic analysis were immediately frozen and stored at −80°C until analysis.

Ertapenem assay. Water and methanol (liquid chromatography-mass spectrometry grade) were purchased from VWR (Darmstadt, Germany); acetic acid, ammonium acetate, and MES were from Sigma-Aldrich (St. Louis, MO, USA); and ertapenem was from Infectopharm (Heppenheim, Germany). The internal standard (meropenem-d$_6$) was purchased from Toronto Research Chemicals (Toronto, Canada). Mobile phase A for high-performance liquid chromatography (HPLC) analysis consisted of water (2 mM ammonium acetate, 0.1% acetic acid, pH 3.8), and mobile phase B was methanol.

The preparation of plasma and dialysate was performed according to the procedures described by Koal et al. (35). Immediately after sampling, MES buffer (0.100 M; pH 6.5; 1:1 [vol/vol]) was added to the samples. Matrix controls, the internal standard, matrix calibration standards, and samples were stored at −80°C until analysis. To every sample, 10 μl of meropenem-d$_6$ in methanol (final concentration, 10 mg/liter) was added as the internal standard. For the preparation of calibration standards and controls for dialysate experiments, MES buffer was used as the matrix. To separate the unbound fraction of ertapenem from the total plasma concentration, an Amicon Ultra Filter ultrafiltration system (molecular mass cutoff, 10 kDa; Millipore, Bedford, MA, USA) was used. Filters were first conditioned by the filtration of 1,000 μl water (40 min, 4,500 × g, 25°C), followed by the ultrafiltration experiment with 100-μl plasma aliquots (40 min, 4,000 × g, 25°C). A volume of 10 μl of an internal standard solution was added to a 50-μl aliquot of each ultrafiltrate sample.

The HPLC system consisted of two pumps (LC 20 AD), an autosampler (SIL 20 AC HT), and an oven (CTO-20 AC) from Shimadzu (Kyoto, Japan). Prepared samples were kept at 4°C in the autosampler until analysis, and the injection volume was 10 μl. Chromatography was performed with an XBridge C$_{18}$ 2.5-μm (3.0- by 75-mm) column (Waters, Milford, MA, USA) in combination with a guard cartridge XBridge C$_{18}$ 2.5-μm (3.0- by 20-mm) column. Separation was performed with a linear gradient (total flow rate, 0.5 ml/min) from minute 0 (95% mobile phase A, 5% mobile phase B) to minute 4 (10% mobile phase A, 90% mobile phase B), followed by a second gradient from minute 4 (10% mobile phase A, 90% mobile phase B) to minute 6 (95% mobile phase A, 5% mobile phase B). A reequilibration of the system was performed for 3 min before the next injection.

An API 3200 triple-quadrupole liquid chromatograph-tandem mass spectrometer (Sciex, Framingham, MA, USA) in the positive electrospray ionization mode (ESI+) was used for mass spectrometry. Analysis was performed using a capillary voltage of 5.0 kV, a temperature of 675°C, a curtain gas pressure of 20 lb/in², a CAD (collisionally activated dissociation) gas pressure of 6 lb/in², gas 1 and 2 at pressures of 55 lb/in², a declustering potential of 36 V, and an entrance potential of 5 V. For ertapenem, we used the transition from m/z 476.0 to m/z 114.0 for quantitative analysis and the transition from m/z 476.0 to m/z 432.5 for qualitative analysis in the multireaction monitoring (MRM) mode. For the internal standard, meropenem-d$_6$, the respective transitions were from m/z 390.1 to m/z 147.2. Analyst software (version 1.6.2) was used for the quantification with linear regression with the origin excluded and 1/x weighting.

The lower limit of quantification (LLOQ; signal-to-noise ratio, >10) for plasma and the dialysate was 0.1 mg/liter. The assay was linear from 0.1 to 100 mg/liter with an r^2 value of 0.998 for the dialysate and an r^2 value of 0.998 for plasma. The interday precision ranged from 4.9 to 12.9% (CV) for the dialysate and 7.5 to 15.7% (CV) for plasma. The intraday precision ranged from 2.5 to 5.2% (CV) for the dialysate and 1.9 to 10.1% (CV) for plasma. The accuracy for plasma was from 89.4 to 107.7%, and that for the

dialysate was 96.7 to 112.8%. For precision and accuracy experiments, five replicates with three concentrations (1, 50, 100 mg/liter) were analyzed.

Population modeling and Monte Carlo simulations. (i) Structural model to describe plasma concentrations. Linear models with one, two, or three disposition compartments were considered to characterize the PK of unbound ertapenem in plasma. A linear binding component and a saturable binding component were used to model the plasma protein binding of ertapenem as we described previously (14, 36).

(ii) Evaluating the rate and extent of tissue penetration. We employed three approaches to characterize the kinetics of tissue penetration. The first approach assumed that the rate of tissue penetration is rapid; i.e., tissue concentrations were assumed to be in equilibrium at the time of the first observation in tissue. For this approach, the unbound tissue concentration was calculated by multiplying the unbound concentration in the central compartment (i.e., plasma) by a factor (F_{SC} for subcutaneous tissue and F_{PF} for peritoneal fluid). F_{SC} and F_{PF} also represent the area under the concentration-time curve (AUC) for unbound concentrations of ertapenem in subcutaneous tissue or peritoneal fluid, respectively, divided by the AUC for unbound concentrations of ertapenem in plasma, as described previously (4, 37).

For the second approach, the tissue sites were assumed to have the same distribution kinetics as the shallow peripheral or the deep peripheral compartment. Therefore, the unbound tissue concentrations were calculated by multiplying the unbound concentration in the shallow peripheral or deep peripheral compartment by F_{SC} and by F_{PF}. F_{SC} and F_{PF} carry the same interpretation as the AUC ratios, as described above. This approach evaluated whether subcutaneous tissue and peritoneal fluid were kinetically more similar to the shallow peripheral compartment or the deep peripheral compartment than to the central compartment (used in the first approach).

The third approach directly estimated the kinetics of tissue penetration. We treated each tissue site as an additional compartment with a small volume of distribution (fixed to 0.1 liter) and estimated the equilibration half-life for each tissue. The small volume was chosen to not affect (or only minimally affect) the disposition parameters of ertapenem estimated on the basis of the plasma concentrations. Details about this approach have been previously described (4, 38). This approach captured the scenario that an equilibrium between tissue and plasma has not yet been reached at the time of collection of the first tissue sample; this approach is the most flexible, as it allowed the rate of equilibration in subcutaneous tissue and peritoneal fluid to differ from the rate of equilibration in the shallow peripheral and deep peripheral compartment. Overall, these three approaches capture the relevant scenarios for the rate and extent of tissue penetration.

(iii) Parameter variability model and covariate effects. Between-subject variability (BSV) was described by log-normal distributions for all model parameters. We applied standard allometric scaling based on WT or FFM to predict the alterations in clearance and volume of distribution between morbidly obese and nonobese patients. In contrast to WT, the FFM (19) accounts for the altered body composition of morbidly obese patients relative to that of nonobese patients. Using the body mass index (BMI), FFM was calculated as (19)

$$\text{FEM (female)} = \frac{9{,}270 \cdot \text{WT}}{8{,}780 + (244 \cdot \text{BMI})} \quad (1)$$

$$\text{FEM (male)} = \frac{9{,}270 \cdot \text{WT}}{6{,}680 + (216 \cdot \text{BMI})} \quad (2)$$

where WT is in kilograms and BMI is in kilograms per square meter.

We did not assess other measures of body size, such as ideal body weight, predicted normal weight (19, 31), or lean body mass, according to the Cheymol and James equation (32, 33), due to the small sample size of our study. Overall, FFM is a plausible and readily available measure of body size (19) which has been previously evaluated for use with obese patients (33). A simulation-estimation study (39) showed that empirical testing for covariate effects is not recommended for studies with less than approximately 50 subjects. Therefore, we did not perform empirical testing for covariate effects.

(iv) Estimation. All population PK model parameters were simultaneously estimated on the basis of all ertapenem concentrations at each site. We used the importance sampling algorithm (pmethod = 4) in parallelized S-ADAPT (version 1.57) software (40) and the SADAPT-TRAN facilitator (41, 42). The Beal M3 method was used for unbound plasma concentrations below the lower limit of quantification (43). Unbound tissue concentrations below the quantification limit were not used during modeling. Models were compared on the basis of the objective function (negative log likelihood), standard diagnostic plots, and the plausibility of the parameter estimates (36, 44, 45); moreover, the predictive performance was carefully assessed by visual prediction checks for each modeled variable (44).

(v) Monte Carlo simulations. On the basis of the final population PK model, Monte Carlo simulations were performed to predict the time course of unbound ertapenem concentrations in plasma, subcutaneous tissue, and peritoneal fluid for morbidly obese patients. For each site and dosing regimen, 1,000 virtual patients were simulated. In the simulations, ertapenem was administered as a 15-min infusion of 1,000 mg every 24 h, as a 15-min infusion of 500 mg every 12 h, or as a continuous infusion of 1,000 g per day (with a 500-mg loading dose).

We simulated morbidly obese patients with the same FFM as those in the present study (geometric mean FFM, 60.3 kg; coefficient of variation, 15.5%). The duration of unbound ertapenem plasma concentrations above the MIC at steady state expressed as a fraction of the dosing interval (fT_{MIC}) was calculated by numerical integration between 24 and 48 h by the use of Berkeley Madonna software (version 8.3.18). The fraction of simulated patients who achieved the PK/PD target values of an fT_{MIC} of 40%, 75%, or 100% was used to approximate the probability of target attainment (46–48). The PD target

of an fT_{MIC} of at least 40% of the dosing interval has been shown to correlate with nearly maximal bacterial killing at 24 h in mice (46, 47). The fT_{MIC} target of 75% has been associated with clinical cure with meropenem in febrile neutropenic patients with bacteremia (49). The fT_{MIC} target of 100% was simulated to predict the PK/PD profile for patients with more severe infections who may need to achieve higher PK/PD targets for successful outcomes. The PK/PD breakpoint was defined as the highest MIC with a probability of target attainment of at least 90%. We compared the PK/PD breakpoints for standard and optimized dosing regimens to the ertapenem MIC data in the EUCAST database (50) for pathogens relevant to infections in morbidly obese patients.

SUPPLEMENTAL MATERIAL

Supplemental material for this article may be found at https://doi.org/10.1128/AAC.00952-16.

TEXT S1, PDF file, 0.5 MB.

ACKNOWLEDGMENTS

We thank Yuanyuan Jiao for support regarding the literature search of this study.

We have no conflict of interest.

REFERENCES

1. Keating GM, Perry CM. 2005. Ertapenem: a review of its use in the treatment of bacterial infections. Drugs 65:1–13. https://doi.org/10.2165/00003495-200565150-00013.
2. Nix DE, Majumdar AK, DiNubile MJ. 2004. Pharmacokinetics and pharmacodynamics of ertapenem: an overview for clinicians. J Antimicrob Chemother 53(Suppl 2):ii23–ii28.
3. Odenholt I. 2001. Ertapenem: a new carbapenem. Expert Opin Investig Drugs 10:1157–1166. https://doi.org/10.1517/13543784.10.6.1157.
4. Wittau M, Scheele J, Kurlbaum M, Brockschmidt C, Wolf AM, Hemper E, Henne-Bruns D, Bulitta JB. 2015. Population pharmacokinetics and target attainment of meropenem in plasma and tissue of morbidly obese patients after laparoscopic intraperitoneal surgery. Antimicrob Agents Chemother 59:6241–6247. https://doi.org/10.1128/AAC.00259-15.
5. Cheatham SC, Fleming MR, Healy DP, Chung EK, Shea KM, Humphrey ML, Kays MB. 2014. Steady-state pharmacokinetics and pharmacodynamics of meropenem in morbidly obese patients hospitalized in an intensive care unit. J Clin Pharmacol 54:324–330. https://doi.org/10.1002/jcph.196.
6. Kays MB, Fleming MR, Cheatham SC, Chung EK, Juenke JM. 2014. Comparative pharmacokinetics and pharmacodynamics of doripenem and meropenem in obese patients. Ann Pharmacother 48:178–186. https://doi.org/10.1177/1060028013512474.
7. Roberts JA, Lipman J. 2013. Optimal doripenem dosing simulations in critically ill nosocomial pneumonia patients with obesity, augmented renal clearance, and decreased bacterial susceptibility. Crit Care Med 41:489–495. https://doi.org/10.1097/CCM.0b013e31826ab4c4.
8. Pletz MW, Rau M, Bulitta J, De Roux A, Burkhardt O, Kruse G, Kurowski M, Nord CE, Lode H. 2004. Ertapenem pharmacokinetics and impact on intestinal microflora, in comparison to those of ceftriaxone, after multiple dosing in male and female volunteers. Antimicrob Agents Chemother 48:3765–3772. https://doi.org/10.1128/AAC.48.10.3765-3772.2004.
9. Hites M, Taccone FS, Wolff F, Maillart E, Beumier M, Surin R, Cotton F, Jacobs F. 2014. Broad-spectrum beta-lactams in obese non-critically ill patients. Nutr Diabetes 4:e119. https://doi.org/10.1038/nutd.2014.15.
10. Laethem T, De Lepeleire I, McCrea J, Zhang J, Majumdar A, Musson D, Rogers D, Li S, Guillaume M, Parneix-Spake A, Deutsch P. 2003. Tissue penetration by ertapenem, a parenteral carbapenem administered once daily, in suction-induced skin blister fluid in healthy young volunteers. Antimicrob Agents Chemother 47:1439–1442. https://doi.org/10.1128/AAC.47.4.1439-1442.2003.
11. Arrigucci S, Garcea A, Fallani S, Cassetta MI, Canonico G, Tonelli F, Mazzei T, Novelli A. 2009. Ertapenem peritoneal fluid concentrations in adult surgical patients. Int J Antimicrob Agents 33:371–373. https://doi.org/10.1016/j.ijantimicag.2008.09.015.
12. Cardone KE, Grabe DW, Kulawy RW, Daoui R, Roglieri J, Meola S, Drusano GL, Lodise TP. 2012. Ertapenem pharmacokinetics and pharmacodynamics during continuous ambulatory peritoneal dialysis. Antimicrob Agents Chemother 56:725–730. https://doi.org/10.1128/AAC.05515-11.
13. Wittau M, Wagner E, Kaever V, Koal T, Henne-Bruns D, Isenmann R. 2006.

Intraabdominal tissue concentration of ertapenem. J Antimicrob Chemother 57:312–316. https://doi.org/10.1093/jac/dki459.
14. Wittau M, Scheele J, Bulitta JB, Mayer B, Kaever V, Burhenne H, Henne-Bruns D, Isenmann R, Brockschmidt C. 2011. Pharmacokinetics of ertapenem in colorectal tissue. Chemotherapy 57:437–448. https://doi.org/10.1159/000333377.
15. Boselli E, Breilh D, Djabarouti S, Bel JC, Saux MC, Allaouichiche B. 2007. Diffusion of ertapenem into bone and synovial tissues. J Antimicrob Chemother 60:893–896. https://doi.org/10.1093/jac/dkm296.
16. Boselli E, Breilh D, Saux MC, Gordien JB, Allaouichiche B. 2006. Pharmacokinetics and lung concentrations of ertapenem in patients with ventilator-associated pneumonia. Intensive Care Med 32:2059–2062. https://doi.org/10.1007/s00134-006-0401-5.
17. Burkhardt O, Kumar V, Katterwe D, Majcher-Peszynska J, Drewelow B, Derendorf H, Welte T. 2007. Ertapenem in critically ill patients with early-onset ventilator-associated pneumonia: pharmacokinetics with special consideration of free-drug concentration. J Antimicrob Chemother 59:277–284.
18. Janson B, Thursky K. 2012. Dosing of antibiotics in obesity. Curr Opin Infect Dis 25:634–649. https://doi.org/10.1097/QCO.0b013e328359a4c1.
19. Janmahasatian S, Duffull SB, Ash S, Ward LC, Byrne NM, Green B. 2005. Quantification of lean bodyweight. Clin Pharmacokinet 44:1051–1065. https://doi.org/10.2165/00003088-200544100-00004.
20. Chen M, Nafziger AN, Drusano GL, Ma L, Bertino JS, Jr. 2006. Comparative pharmacokinetics and pharmacodynamic target attainment of ertapenem in normal-weight, obese, and extremely obese adults. Antimicrob Agents Chemother 50:1222–1227. https://doi.org/10.1128/AAC.50.4.1222-1227.2006.
21. Borracci T, Adembri C, Accetta G, Berti J, Cappellini I, Lucchese M, Biggeri A, De Gaudio AR, Novelli A. 2014. Use of the parenteral antibiotic ertapenem as short term prophylaxis in bariatric surgery: a pharmacokinetic-pharmacodynamic study in class III obese female patients. Minerva Anestesiol 80:1005–1011.
22. Baker MA, Schneider EK, Huang JX, Cooper MA, Li J, Velkov T. 28 September 2016. The plasma protein binding proteome of ertapenem: a novel compound-centric proteomic approach for elucidating drug-plasma protein binding interactions. ACS Chem Biol. https://doi.org/10.1021/acschembio.6b00700.
23. World Health Organization. 2015. Global database on body mass index 2015. World Health Organization, Geneva, Switzerland. http://apps.who.int/bmi/index.jsp.
24. Fischer MI, Dias C, Stein A, Meinhardt NG, Heineck I. 2014. Antibiotic prophylaxis in obese patients submitted to bariatric surgery. A systematic review. Acta Cir Bras 29:209–217. https://doi.org/10.1590/S0102-86502014000300010.
25. Schug-Pass C, Geers P, Hugel O, Lippert H, Kockerling F. 2010. Prospective randomized trial comparing short-term antibiotic therapy versus standard therapy for acute uncomplicated sigmoid diverticulitis. Int J Colorectal Dis 25:751–759. https://doi.org/10.1007/s00384-010-0899-4.
26. Falagas ME, Peppas G, Makris GC, Karageorgopoulos DE, Matthaiou DK.

2008. Meta-analysis: ertapenem for complicated intra-abdominal infections. Aliment Pharmacol Ther 27:919–931. https://doi.org/10.1111/j.1365-2036.2008.03642.x.

27. Burkhardt O, Derendorf H, Welte T. 2007. Ertapenem: the new carbapenem 5 years after first FDA licensing for clinical practice. Expert Opin Pharmacother 8:237–256. https://doi.org/10.1517/14656566.8.2.237.

28. Burkhardt O, Brunner M, Schmidt S, Grant M, Tang Y, Derendorf H. 2006. Penetration of ertapenem into skeletal muscle and subcutaneous adipose tissue in healthy volunteers measured by in vivo microdialysis. J Antimicrob Chemother 58:632–636. https://doi.org/10.1093/jac/dkl284.

29. Sauermann R, Burian B, Burian A, Jager W, Hoferl M, Stella A, Theurer S, Riedl M, Zeitlinger M. 2013. Tissue pharmacokinetics of ertapenem at steady-state in diabetic patients with leg infections. J Antimicrob Chemother 68:895–899. https://doi.org/10.1093/jac/dks479.

30. Boyadjiev I, Boulamery A, Simon N, Martin C, Bruguerolle B, Leone M. 2011. Penetration of ertapenem into muscle measured by in vivo microdialysis in mechanically ventilated patients. Antimicrob Agents Chemother 55:3573–3575. https://doi.org/10.1128/AAC.00180-11.

31. Janmahasatian S, Duffull SB, Chagnac A, Kirkpatrick CM, Green B. 2008. Lean body mass normalizes the effect of obesity on renal function. Br J Clin Pharmacol 65:964–965. https://doi.org/10.1111/j.1365-2125.2008.03112.x.

32. Green B, Duffull SB. 2004. What is the best size descriptor to use for pharmacokinetic studies in the obese? Br J Clin Pharmacol 58:119–133. https://doi.org/10.1111/j.1365-2125.2004.02157.x.

33. Han PY, Duffull SB, Kirkpatrick CM, Green B. 2007. Dosing in obesity: a simple solution to a big problem. Clin Pharmacol Ther 82:505–508. https://doi.org/10.1038/sj.clpt.6100381.

34. Stahle L, Arner P, Ungerstedt U. 1991. Drug distribution studies with microdialysis. III. Extracellular concentration of caffeine in adipose tissue in man. Life Sci 49:1853–1858.

35. Koal T, Deters M, Resch K, Kaever V. 2006. Quantification of the carbapenem antibiotic ertapenem in human plasma by a validated liquid chromatography-mass spectrometry method. Clin Chim Acta 364:239–245. https://doi.org/10.1016/j.cccn.2005.07.004.

36. Bulitta JB, Zhao P, Arnold RD, Kessler DR, Daifuku R, Pratt J, Luciano G, Hanauske AR, Gelderblom H, Awada A, Jusko WJ. 2009. Mechanistic population pharmacokinetics of total and unbound paclitaxel for a new nanodroplet formulation versus Taxol in cancer patients. Cancer Chemother Pharmacol 63:1049–1063. https://doi.org/10.1007/s00280-008-0827-2.

37. Landersdorfer CB, Kinzig M, Hennig FF, Bulitta JB, Holzgrabe U, Drusano GL, Sorgel F, Gusinde J. 2009. Penetration of moxifloxacin into bone evaluated by Monte Carlo simulation. Antimicrob Agents Chemother 53:2074–2081. https://doi.org/10.1128/AAC.01056-08.

38. Landersdorfer CB, Kinzig M, Bulitta JB, Hennig FF, Holzgrabe U, Sorgel F, Gusinde J. 2009. Bone penetration of amoxicillin and clavulanic acid evaluated by population pharmacokinetics and Monte Carlo simulation.

Antimicrob Agents Chemother 53:2569–2578. https://doi.org/10.1128/AAC.01119-08.

39. Ribbing J, Jonsson EN. 2004. Power, selection bias and predictive performance of the population pharmacokinetic covariate model. J Pharmacokinet Pharmacodyn 31:109–134. https://doi.org/10.1023/B:JOPA.0000034404.86036.72.

40. Bauer RJ, Guzy S, Ng C. 2007. A survey of population analysis methods and software for complex pharmacokinetic and pharmacodynamic models with examples. AAPS J 9:E60–E83. https://doi.org/10.1208/aapsj0901007.

41. Bulitta JB, Bingolbali A, Shin BS, Landersdorfer CB. 2011. Development of a new pre- and post-processing tool (SADAPT-TRAN) for nonlinear mixed-effects modeling in S-ADAPT. AAPS J 13:201–211. https://doi.org/10.1208/s12248-011-9257-x.

42. Bulitta JB, Landersdorfer CB. 2011. Performance and robustness of the Monte Carlo importance sampling algorithm using parallelized S-ADAPT for basic and complex mechanistic models. AAPS J 13:212–226. https://doi.org/10.1208/s12248-011-9258-9.

43. Beal SL. 2001. Ways to fit a PK model with some data below the quantification limit. J Pharmacokinet Pharmacodyn 28:481–504. https://doi.org/10.1023/A:1012299115260.

44. Bulitta JB, Duffull SB, Kinzig-Schippers M, Holzgrabe U, Stephan U, Drusano GL, Sorgel F. 2007. Systematic comparison of the population pharmacokinetics and pharmacodynamics of piperacillin in cystic fibrosis patients and healthy volunteers. Antimicrob Agents Chemother 51:2497–2507. https://doi.org/10.1128/AAC.01477-06.

45. Bulitta JB, Okusanya OO, Forrest A, Bhavnani SM, Clark K, Still JG, Fernandes P, Ambrose PG. 2013. Population pharmacokinetics of fusidic acid: rationale for front-loaded dosing regimens due to autoinhibition of clearance. Antimicrob Agents Chemother 57:498–507. https://doi.org/10.1128/AAC.01354-12.

46. Craig WA. 1998. Pharmacokinetic/pharmacodynamic parameters: rationale for antibacterial dosing of mice and men. Clin Infect Dis 26:1–12. https://doi.org/10.1086/516284.

47. Ambrose PG, Bhavnani SM, Rubino CM, Louie A, Gumbo T, Forrest A, Drusano GL. 2007. Pharmacokinetics-pharmacodynamics of antimicrobial therapy: it's not just for mice anymore. Clin Infect Dis 44:79–86. https://doi.org/10.1086/510079.

48. Bulitta JB, Landersdorfer CB, Forrest A, Brown SV, Neely MN, Tsuji BT, Louie A. 2011. Relevance of pharmacokinetic and pharmacodynamic modeling to clinical care of critically ill patients. Curr Pharm Biotechnol 12:2044–2061. https://doi.org/10.2174/138920111798808428.

49. Ariano RE, Nyhlen A, Donnelly JP, Sitar DS, Harding GK, Zelenitsky SA. 2005. Pharmacokinetics and pharmacodynamics of meropenem in febrile neutropenic patients with bacteremia. Ann Pharmacother 39:32–38.

50. European Committee on Antimicrobial Susceptibility Testing (EUCAST). 2016. Antimicrobial wild type distributions of microorganisms. http://www.escmid.org/research_projects/eucast. Accessed 5 September 2016.